Distances From Capillaries to Arterioles or Venules Measured Using OCTA and AOSLO

Edmund Arthur,[1] Ann E. Elsner,[1] Kaitlyn A. Sapoznik,[1] Joel A. Papay,[1] Matthew S. Muller,[2] and Stephen A. Burns[1]

[1]Indiana University School of Optometry, Bloomington, Indiana, United States
[2]Aeon Imaging, LLC, Bloomington, Indiana, United States

Correspondence: Ann E. Elsner, Indiana University School of Optometry, 800 East Atwater Avenue, Bloomington, IN 47405-3860, USA; aeelsner@indiana.edu.

Submitted: July 16, 2018
Accepted: March 29, 2019

Citation: Arthur E, Elsner AE, Sapoznik KA, Papay JA, Muller MS, Burns SA. Distances from capillaries to arterioles or venules measured using OCTA and AOSLO. *Invest Ophthalmol Vis Sci*. 2019;60:1833–1844. https://doi.org/10.1167/iovs.18-25294

Purpose. To investigate distances from retinal capillaries to arterioles or venules noninvasively.

Methods. An adaptive optics scanning laser ophthalmoscope (AOSLO) and optical coherence tomography angiography (OCTA) imager acquired detailed maps of retinal vasculature. Using OCTA, we quantified the distance from the edge of an arteriole or venule to the middle of the nearest capillaries (periarteriole or perivenule capillary-free zones, respectively) within the superficial vascular plexus of 20 young healthy subjects with normal axial lengths. These distances were compared to AOSLO images for three subjects. We tested the relation between the peripheral capillary-free zones and FAZ horizontal, vertical, effective diameters, and asymmetry indices in the deep vascular plexus. We examined enlargement with OCTA of capillary-free zones in a type 2 diabetic patient.

Results. The periarteriole capillary-free zone (67.2 ± 25.3 μm) was readily visible and larger than the perivenule capillary-free zone (42.7 ± 14.4 μm), $F_{(1,\ 998)} = 771$, $P < 0.0001$. The distance from foveal center ($P = 0.003$) and diameter ($P = 0.048$) were predictive of perivenule capillary-free zone values. OCTA and AOSLO corresponded for arterioles. FAZ effective diameter was positively associated with asymmetry indices, $r = 0.49$, $P = 0.028$, but not peripheral capillary-free zones, although focal enlargements were found in a diabetic patient.

Conclusions. For normal retinas, periarteriole and perivenule capillary-free zones are readily visible with OCTA and AOSLO. Periarteriole capillary-free zones were larger, consistent with arterioles carrying oxygen rich blood that diffuses to support the retina.

Keywords: foveal avascular zone, periarteriole capillary-free zone, perivenule capillary-free zone, OCT angiography, adaptive optics scanning laser ophthalmoscopy

Retinal capillaries are the key interface for the exchange of nutrients, oxygen, and metabolites between retinal neurons and the vascular system.[1] The retinal neurovascular unit consists of blood vessel endothelial cells, pericytes, astrocytes, Müller cells, and neurons that are intimately connected to form the inner blood-retinal barrier that controls nutrient flow to the neural retina.[2] A capillary-free zone, represents the maximum distance that nutrients and oxygen must travel to reach the retinal neurons. Thus, the diffusion distance would be half or less depending on the location of the neural element or Müller cell to the capillary, arteriole or venule.

Capillary-free zones in the retina can now be mapped with noninvasive methods, using the motion over time of the red blood cells computed across a series of images, using adaptive optics scanning laser ophthalmoscopy (AOSLO)[3] or optical coherence tomography angiography (OCTA).[4,5] The comparison of AOSLO maps of the foveal avascular zone (FAZ) to noninvasive retinal thickness measurements from OCT shows that in the normal retina, the inner retinal layers have a relatively constant thickness at the margins of the FAZ; and for this particular neural and glial tissue, retinal capillaries are needed to sustain an inner retinal thickness greater than 60 μm.[6] Greater distances may indicate potential ischemia or a very sick retina with a decreased oxygen demand, found in diseases such as diabetic retinopathy (DR) when the distribution and structure of capillaries are altered including poor perfusion, or dropout of capillaries and vessel remodeling.[7–11]

Slowed perfusion or dropout of capillaries are both well-documented in vivo in DR by the early phase measurements of fluorescein angiography (FA). These measurements show changes for both FAZ and parafoveal regions for diameter, asymmetry, pore size, or other measurements of capillary spacing.[12–18] Invasive methods for visualizing capillaries include histology,[19] FA,[12,18,20,21] and indocyanine green angiography (ICGA).[22] Noninvasive methods include OCTA[5,23–27] and AOSLO,[3] the adaptive optics digital light ophthalmoscope (AODLO),[28] and the subjective blue field entoptoscope technique that agrees well with FA.[29] The FAZ is also quantified noninvasively using transverse analysis of layer reflectivity and geometry of the foveal pit, using spectral domain OCT (SD-OCT).[30] Due to the lack of axial resolution for all techniques other than AOSLO, AODLO, and OCTA, assessment of more peripheral capillary-free zones can be problematic unless the retina is thin or there is minimal dye leakage.

Regardless of measurement method, there is large inter-individual variability in the FAZ size[6,12,18,20,23–26,30] that is related to large variability in foveal morphology. As a result, FAZ size measured for even a diabetic patient with capillary loss is

not always significantly greater compared to controls.[7,30] Some studies on the interaction of FAZ size with aging show an increase, but with differing quantitative characterization for FA[18,21] and OCTA.[24,26] In contrast, other studies show no significant increase, perhaps due to insufficient statistical power, or lack of analysis with FA,[12,20] histology,[19] and OCTA.[23,25] In normal eyes, FAZ shape is horizontally elongated with a large FAZ size and vertically elongated with a small FAZ size.[6]

Another difficulty in using FAZ size to assess the status of the fovea or manage a diabetic patient is that the measurement per se is limited to only a few capillaries. In the case of severe DR, a metric of size increase may saturate, with no possibility of further size increase with increasing disease. FAZ capillaries are limited to the deeper layers because of the foveal pit, and are located only near the fovea where there is little influence of the ganglion cells. In contrast, assessing the status of the peripheral retina and the featureless retina, and not limiting assessment to visible vascular changes have been important clinical concepts for decades.[31] Hence, in order to help in the diagnosis and management of DR, the use of salient features, such as black regions on OCTA next to a clearly visible and bright arteriole or venule, and more peripheral features could produce a more sensitive biomarker when used either alone or combined with FAZ metrics.

There are numerous capillary-free zones around larger blood vessels outside the fovea that could be used to help detect early damage to retinal vasculature. These have been demonstrated in living adult retinas using FA[32,33] and histology[34,35] when resolved in 3D. Capillary-free zones outside the fovea were imaged noninvasively, shown to be salient features, and comparable when acquired with AOSLO and OCTA (Muller MS, et al. *IOVS 2017*;58:ARVO E-Abstract 2003). These capillary-free zones are a part of the normal vascular development process, when there is retraction or atrophy of the capillaries surrounding developing larger retinal vessels (i.e., arterial and venous channels develop while some of the side branches retract and atrophy).[36] The presence of a capillary-free zone around the arterioles, the periarteriole capillary-free zone, may develop as a result of a vasoinhibitory effect of oxygen diffusing out of the retinal arterioles.[32] The oxygen saturation within retinal arteries (77.8%–94.3%) is higher than in veins (55.5%–71.4%), but nevertheless for veins, the oxygen saturation and oxygen content are >50% that of arteries.[37] Together with the fact that veins are typically larger than arteries, these measurements of veins imply that veins provide a potential source of oxygen for neighboring neural and glial tissues. The lesser amount of oxygen in venules is consistent with a narrower capillary-free zone around the venules, the perivenule capillary-free zone that has been demonstrated with histology.[34]

Both OCTA and AOSLO have sufficient axial resolution to resolve the superficial retinal capillaries adjacent to larger arterioles and venules. A key underlying difference between AOSLO and OCTA is the significantly better lateral resolution of AOSLO (2 μm), but worse axial resolution of AOSLO (>40 μm). AOSLO provides diffraction limited images of the retina by correcting the optical imperfections of the eye with a deformable mirror.[3,7,38] OCTA has worse lateral resolution, with a pixel typically wider than a capillary, but better axial resolution (<10 μm axial resolution). Capillaries are visualized in individual images with AOSLO, without needing flow, therefore distinguishing capillary-free zones from capillaries with slow flow, which have been confused with OCTA.[35] A second difference is the field of view, which in AOSLO is usually limited to an isoplantic patch of a few degrees visual angle, but OCTA has a variable field of view up to 10 to 20°. More AOSLO samples, and therefore more data collection and processing time, are usually needed to cover a wide area of retina. A third difference is that particle motion seen only in AOSLO videos can help distinguish vessels from noise or indicate the direction of flow, distinguishing arteries from veins.[3] A fourth difference is that OCTA analyses use post-processing to obtain segmentation of retinal layers to assign motion to different vascular plexuses. Noise in the measurements of the deeper layers due to motion, absorption, and reflections in the overlying layers is known as projection artifact and is an area of ongoing technique development.[5] The superficial and deep vascular plexuses (SVP and DVP), have been generated using nonprojection resolved OCTA,[4,39] while the superficial, intermediate, deep, and the peripapillary vascular plexuses have been generated using projection resolved OCTA.[40–42] ICGA, OCTA, and AOSLO typically use near infrared wavelengths, which cause fewer artifacts from anterior segment media issues, foveal melanin, and macular pigment than the shorter wavelengths used with FA.[43]

An updated clinical classification of DR is emerging, since it is well-established that there can be retinal vascular remodeling and functional changes more severe than indicated by clinical exam or fundus photography,[7,38,44] and these can be quantified.[27,40,45,46] The capillary-free zones could provide a salient clinical sign, as well as a quantitative biomarker for tissue oxygenation when measured as the linear distance between the edge of an arteriole or venule and the nearest capillaries. Greater distances indicate potential ischemia in diabetic patients. Capillary-free zones from the periphery could be combined with FAZ metrics to help in the detection and management of DR.[5,45,46]

In this paper, we quantify the width of periarteriole and perivenule capillary-free zones using OCTA and AOSLO in young healthy subjects who do not have high refractive errors, and investigate the effect of sex as well as provide evidence of potential remodeling in diabetic patients. We examined the association between the metrics for the more peripheral periarteriole and perivenule capillary-free zones and the central macular FAZ, which are hypothesized to provide similar information; the association is expected to be weakened in normal subjects due to interindividual differences in foveal development.

Methods

Subjects

Young, healthy subjects (10 males and 10 females) free of ocular disease were recruited for this study. The estimated sample size was computed with a GPower 3.1 calculator using the following input parameters; effect size (partial eta squared) of 0.28, α of 0.05, power of 0.80, 3 independent variables (sex, vessel type, distance from fovea), and two levels for sex and vessel type.[47] All subjects had refractive error $< \pm 3.00$ diopters (D) to prevent significant differences in retinal magnification. Further exclusion criteria were lack of systemic disease or uncontrolled blood pressure. Axial length measurements were taken with the biometer (IOLMaster, version 5; Carl Zeiss Meditec, Dublin, CA, USA). The mean age of males (27.0 ± 3.02 years) and females (25.6 ± 3.13 years) did not differ, $t(18) = 1.02$, $P = 0.32$. There was no statistically significant difference between the mean axial length of males (23.8 ± 0.824 mm) and females (23.5 ± 0.847 mm), $t(18) = 0.83$, $P = 0.42$. To show remodeling of the capillary-free zones in diabetics, we also included data from a type 2 diabetic female, 54 years, duration of 11 years, and HbA1c of 8.0. Visual acuity was 20/20 – 2 OD, but the patient demonstrated that improvement could be made with pinhole OS from 20/60 + 2

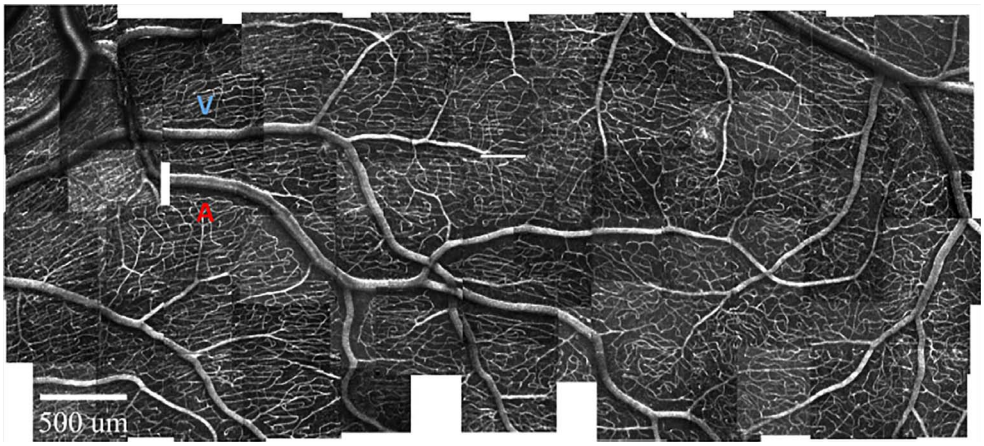

Figure 1. AOSLO montage of a 30-year-old healthy female showing detailed peripheral vasculature of a paired arteriole, venule, and surrounding capillaries of the SVP. Regions free of capillaries are clearly seen around the arteriole (periarteriole capillary-free zone) and venule (perivenule capillary-free zone). The periarteriole capillary-free zone can be observed as wider than the perivenule capillary-free zone. For both capillary-free zones, a wide selection of regions of interests were used for measurements. A paired arteriole and venule are labeled "A" and "V," respectively. The AOSLO images have spatial resolution sufficient to provide several pixels across each capillary. Although following the blood flow through the microvascular network requires the video sequence, there is a clear demonstration of the branching of arterioles but not capillaries off the arteries, occurring at intervals much greater than a capillary pore (i.e., the spaces between the capillaries). The arterioles appear wider in the motion map and brighter than capillaries because of higher blood flow. The capillaries, which can be as much as the 5th branches, tile the retina in a network across the retina having much larger pores than the width of the lumen of capillaries. The capillaries feed into venules, which can be seen as the brighter structures that intersect with the veins, again at much larger intervals than the size of a capillary pore. Next to both arteries and veins, there can be long distances of capillary pores being parallel to the larger vessel, but not connecting with them. The capillaries can have elongated pores (next to the blue "V" or above the artery just before the artery and vein cross to the right of the symbols) and sometimes run beneath the veins.

to 20/20 – 1. This patient had a thin retina despite having small cysts and vitreoretinal traction, e.g., the central macular thickness on OCT (Spectralis, Heidelberg Engineering, Heidelberg, Germany) was only 229 ± 0.18 μm, with the inner ETDRS ring, 275, 244, 236, 269 and outer ETDRS ring, 257, 271, 243, and 243 μm for temporal, superior, nasal, and inferior retina, respectively. As the superficial vascular plexus was under study for controls for the peripheral capillary-free zones, but the patient had the potential for segmentation error because of the traction, we analyzed the sum of both the plexuses. This provides a conservative estimate of the size of the peripapillary arteriole and venule capillary-free zones, (i.e., the lower bound of the capillary-free zones). The study adhered to the tenets of the Declaration of Helsinki, and informed consent from all subjects was obtained prior to experimental data collection after explanation of the nature and possible consequences of the study. The study was approved by the Indiana University Institutional Review Board (IRB).

Imaging Session with AOSLO

Videos (30 frames/second) of paired arterioles, venules, and surrounding capillaries of the SVP of 3 subjects (ages 27, 29, and 30 years) were acquired with a point scanning AOSLO at 0.93 μm/pixel and wavelengths of 775 ± 20 and 827 ± 20 nm.[48] Different confocal apertures were used in the two optical imaging channels to visualize vessel walls versus lumen to obtain accurate vessel widths[49] or emphasize reflectivity of flowing particles versus absorption in the arterioles for motion mapping for capillary density.[48] Videos were processed using custom software (MATLAB; MathWorks, Natick, MA, USA)[50] and perfusion maps were generated using the variance of scatter from moving blood flow.[51] The variance maps were montaged in image editing software (Photoshop CS6; Adobe, Inc., San Jose, CA, USA) to generate a wider field of view of the paired arterioles, venules, and surrounding capillaries, which provides the potential for numerous regions of interest to be measured (Fig. 1). For illustrative purposes only, vessels were manually traced using a single pixel pencil tool in image editing software (Adobe, Inc.), using a 27-inch graphics tablet and electronic pen (Cintiq, WACOM, Portland, OR, USA) to better illustrate the relative locations of all vessels, and the periarteriole and perivenule capillary-free zones (Fig. 2). Distances between capillaries and the arterioles and lumen widths were computed manually from the images, not the tracing, using the image editing software (Adobe, Inc.) measurement tool and compared with OCTA measurements.

Imaging Session with OCTA

OCTA images of paired arterioles and venules with their surrounding capillaries were obtained (Spectralis HRA + OCT; Eye Explorer version 1.9.14.0 software with upgrades through 1.9.17.0; Heidelberg Engineering). The signal quality values of all our OCTA images from the vendor software ranged from 30 to 40 with 40 being the highest possible value that can be obtained. For all subjects, we analyzed the SVP in an approximately linear pattern evenly along each sampled arteriole or venule. The average distances from the fovea of the regions of interest were 14.2° ± 3.22° (range 8.28°–19.6°) and 14.6° ± 2.39° (range: 10.7°–20.4°), respectively for arterioles and venules. The distance from the foveal center for arterioles (14.7° ± 2.57°) and venules (14.4° ± 3.03°) for males did not differ from the arteriole (13.8° ± 3.85°) and venule (14.7° ± 1.71°) distance from the foveal center for females, $t(18) = 0.619$, $p = 0.54$, $t(18) = -0.221$, $P = 0.83$ for arterioles and venules, respectively. The SVP was defined as the retinal vasculature from the inner limiting membrane (ILM) to the inner plexiform layer (IPL)/inner nuclear layer (INL) boundary while the DVP consisted of the retinal vasculature from the IPL/INL boundary to the outer plexiform layer (OPL)/outer nuclear layer (ONL) boundary. Each OCTA image was 10 × 10° consisting of 512 b-scans, 512 A-scans per b-scan, 6-μm spacing between the b-scans and seven frames averaged per each b-scan location. Images were then manually montaged

Investigative Ophthalmology & Visual Science

Figure 2. Tracing of the AOSLO montage from Figure 1 for a 30-year-old healthy female showing arterioles, venules, and capillaries of the SVP using a single pixel pencil in an image editing program (Adobe, Inc.). Regions free of capillaries are better delineated around the arteriole (periarteriole capillary-free zone) and venule (perivenule capillary-free zone). The periarteriole capillary-free zone can be observed as wider than the perivenule capillary-free zone. Paired arteriole and venule are labeled "A" and "V" respectively.

using image editing software (Adobe, Inc.) to generate a wider field of view of the paired vessels (Fig. 3).

Image Analysis

Computation of Periarteriole and Perivenule Capillary-Free Zones in OCTA Images. To compute the distance from the vessel to the capillary, we calculated the length of a line, drawn perpendicular to the arteriole or venule, between the nearest edge of the larger vessel and the center of the capillary, using the SVP (Fig. 4). The middle of the nearest capillary and not the edge was chosen because OCTA does not have sufficient lateral resolution to accurately delineate the edge of a capillary. Multiple distance samples were collected by manual marking at close spacing, so that orientation or curvature artifacts were negligible. A custom computing program (MathWorks, Inc.) then automatically recorded the x and y coordinates of each marked point and saved these values in spreadsheet software (Microsoft Excel 2013; Microsoft Corp., Redmond, WA, USA) files. Each distance sample was then computed as distance $= [(X_{\text{large vessel edge}} - X_{\text{capillary}})^2 + (Y_{\text{large vessel edge}} - Y_{\text{capillary}}{}^2]\text{^}^{1/2}$. The number of pixels computed was then converted into microns by multiplying the Euclidean distances by the micron-to-pixel ratio in the x and y directions, as computed from the fiducial marks (Heidelberg Engineering). The periarteriole and perivenule capillary-free zones were then computed as the average of 50 Euclidean distance samples.

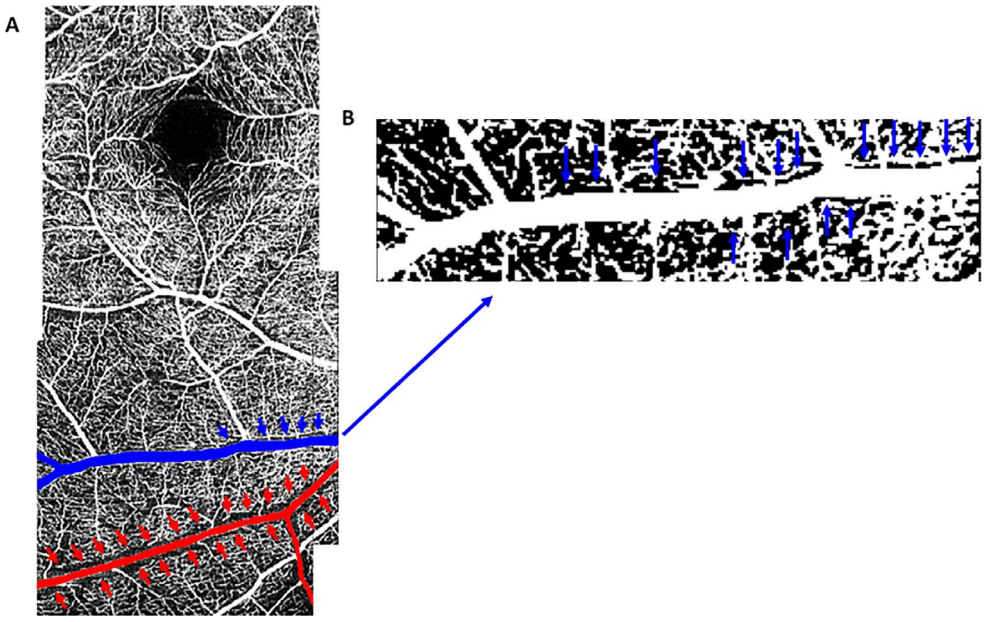

Figure 3. OCTA montage of $10^\circ \times 10^\circ$ images plus enlargement of the venule portion of a 30-year-old healthy male showing paired arteriole (*red*) and venule (*blue*) at 13.7° and 11.9°, respectively, from the foveal center in the SVP. (**A**) Periarteriole and perivenule capillary-free zones indicated by *blue* and *red arrows*, respectively. SVP consists of retinal vasculature from the ILM to the IPL/INL boundary. (**B**) Magnified binarized image of the venule showing well-defined narrow perivenule capillary-free zones. Periarteriole capillary-free zone can be observed as wider than the perivenule capillary-free zone in (**A**).

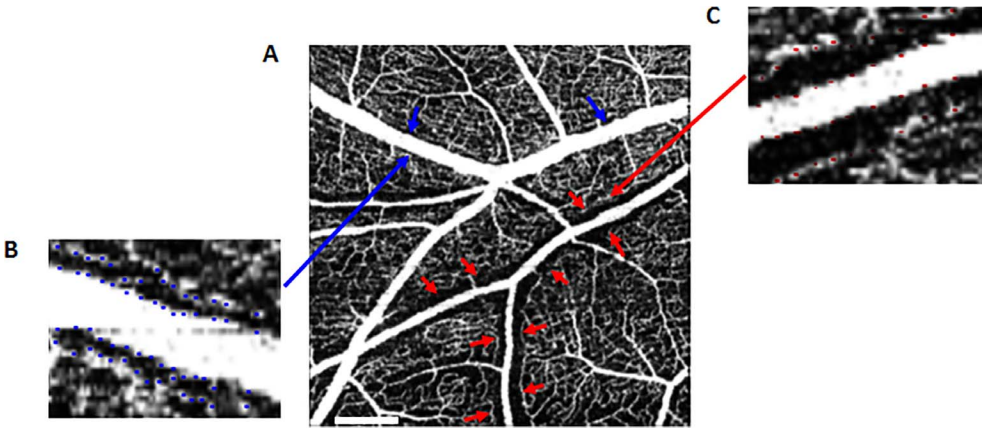

Figure 4. OCTA image of a 22-year-old healthy male showing marking and computation of periarteriole and perivenule capillary-free zones in the SVP. (**A**) A single 10° × 10° OCTA image showing a paired venule (bigger of the two vessels) and arteriole (smaller of the two vessels) at 10.7° and 12.5°, respectively inferior from the foveal center. *Red* and *blue arrows* show the periarteriole and perivenule capillary-free zones, respectively. (**B**) Enlarged portion of the venule showing the markings (*blue*) of the venule top, bottom, and middle of capillaries at the venule top and bottom. (**C**) Enlarged portion of the arteriole showing the markings (*red*) of the arteriole top, bottom, and middle of capillaries at the arteriole top and bottom. Periarteriole capillary-free zones can be seen as wider than perivenule capillary-free zones. *Scale bar*: 500 µm.

Computation of Arteriole Diameter, Venule Diameter, and Distance From Foveal Center in OCTA Images. The paired arteriole or venule lumen diameter was computed as $[(X_{\text{vessel top}} - X_{\text{vessel bottom}})^2 + (Y_{\text{vessel top}} - Y_{\text{vessel bottom}})^2]\text{^}^{1/2}$. To compute arteriole and venule distance from the center of the fovea, the center of the FAZ was marked and corresponding x and y coordinates generated. The vessel distance from the center of the fovea was then computed as $[(X_{\text{vessel top}} - X_{\text{fovea}})^2 + (Y_{\text{vessel top}} - Y_{\text{fovea}})^2]\text{^}^{1/2}$. The number of pixels computed was then converted into microns by multiplying them by the micron to pixel ratio in the x and y directions from the vendor's fiducial marks and then converted into degrees.

Computation of FAZ size, and Asymmetry Index in OCTA Images. Using vendor software, the FAZ of all subjects in the DVP was marked and the area covered recorded (Fig. 5A). The horizontal FAZ diameter (FAZ_H) and the vertical FAZ diameter (FAZ_V) were also computed (Fig. 5B). Asymmetry indices was then computed as the ratio of FAZ_H to FAZ_V (FAZ_H/FAZ_V). A second method for FAZ diameter was computed from the FAZ area values, defined as the diameter of the circle whose area was equivalent to the area of the FAZ (the effective diameter). Hence, the FAZ effective diameter = $(4\text{*FAZ area}/\pi)^{1/2}$.

Statistical Analysis

All statistical analyses were performed using statistical software (IBM SPSS Statistics for Windows, Version 24.0; IBM Corp., Armonk, NY, USA). All values are presented as mean ± SD. Samples included 50 points of periarteriole and perivenule capillary-free zones for each subject, sampled evenly at regular intervals or equally spaced along a linear distance of 1.78 ± 1.12 mm and 1.38 ± 0.717 mm for arterioles and venules, respectively, for statistical analysis. A 2 × 2 mixed model ANOVA was performed with sex (male and female) and vessel type (arteriole and venule) as independent variables and width of capillary-free zone as the dependent variable. A multiple linear regression of periarteriole capillary-free zone as the dependent variable versus arteriole distance from foveal center, arteriole diameter, and sex as predictors was performed. A multiple linear regression of perivenule capillary-free zone as the dependent variable versus venule distance from foveal center, venule diameter, and sex as predictors was also performed. The mean periarteriole and perivenule capillary-free zones were computed. The associations between the mean periarteriole capillary-free zone versus FAZ effective diameter, mean perivenule capillary-free zone versus FAZ effective diameter, mean periarteriole capillary-free zone

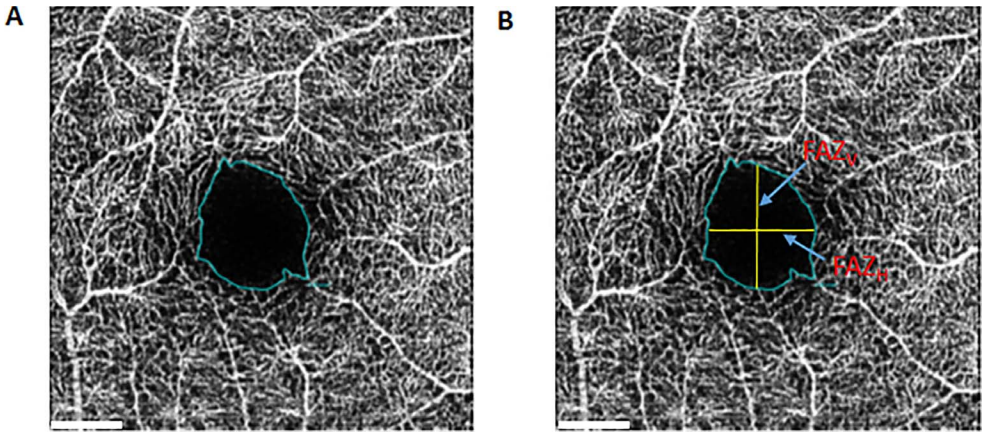

Figure 5. OCTA 10° × 10° image of a 24-year-old healthy male showing marked FAZ and asymmetry indices. (**A**) DVP showing a marked FAZ area of 0.49 mm^2. (**B**) DVP showing the FAZ_H and FAZ_V. Asymmetry indices is computed as FAZ_H/FAZ_V. *Scale bar*: 500 µm.

Investigative Ophthalmology & Visual Science

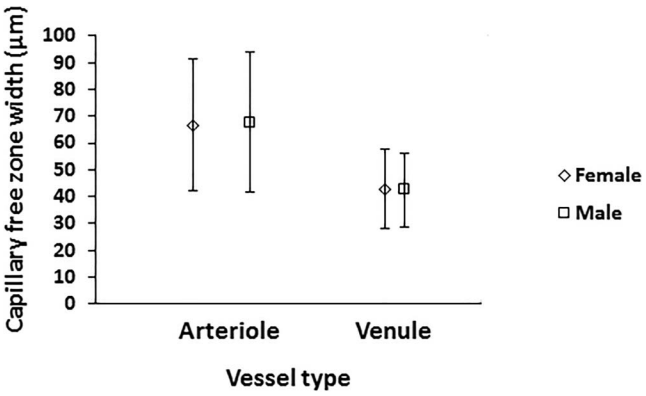

FIGURE 6. The effect of vessel type and sex on the width of capillary-free zone. The periarteriole capillary-free zone is larger than the perivenule capillary-free zone for both males and females ($P < 0.0001$). There is no significant interaction between vessel type and sex on the width of the capillary-free zones ($P = 0.41$). Males had similar periarteriole and perivenule capillary-free zones compared to females ($P = 0.72$). *Error bars* represent standard deviation.

versus mean perivenule capillary-free zone, asymmetry indices versus FAZ effective diameter, and FAZ size versus age were examined using Pearson product moment correlation. Independent *t*-tests were used to compare the means of the FAZ metrics and the various covariates between males and females, assuming Levene's test for equality of variance was not statistically significant. An F test for two sample variances compared the intersubject variability of periarteriole vs. perivenule capillary-free zones, periarteriole capillary-free zone versus FAZ size, and perivenule capillary-free zone versus FAZ size. A value of $P < 0.05$ was considered statistically significant.

RESULTS

The periarteriole and perivenule capillary-free zones were readily computed for both AOSLO and OCTA methods for all 3 subjects. The AOSLO, which has the spatial resolution to provide measurements of the walls as well as the lumens, gave an average width of the arteriole lumens of 68.0 ± 5.00, 69.0 ± 3.00, and 53.0 ± 2.00 μm, with a wall: lumen ratio of 0.265, 0.688, and 0.781, similar to previous findings.[49] The flow through the lumen is visualized for both AOSLO and OCTA, but walls are visualized by AOSLO only. The AOSLO and OCTA values agreed for the periarteriole capillary-free zones. Measuring at similar distances from the fovea (Fig. 1) (12.3°, 15.3°, and 13.7°, respectively), the distance from the lumen to the nearest capillary loop for AOSLO was 59.0 ± 21.0, 50.0 ± 17.0, and 55.0 ± 15.0 μm and from the edge of the vessel to the capillary with OCTA was 53.0 ± 16.0, 51.0 ± 20.0, and 52.0 ± 15.0 μm, for each of the three subjects, respectively. Subsequent results are reported only from the OCTA images, which provided data across a wide field in a time efficient manner.

For measurements using OCTA, in the SVP, the width of the periarteriole capillary-free zone (67.2 ± 25.3 μm) was significantly greater than that of the perivenule capillary-free zone (42.7 ± 14.4 μm), $F_{(1, 998)} = 771$, $P < 0.0001$ (Fig. 6). No difference was found in the sample for the mean arteriole diameter of males (99.8 ± 11.5 μm) and females (105 ± 15.3μm), $t(18) = -0.805$, $P = 0.43$. Similarly, the mean venule diameter of sampled vessels did not differ for males (129 ± 18.9 μm) and females (129 ± 20.7 μm), $t(18) = 0.056$, $P = 0.96$. There was no significant interaction between vessel type and sex on the width of the capillary-free zone, $F_{(1, 998)} = 0.684$, $P = 0.41$ (Fig. 6). Males had similar periarteriole capillary-free zone (67.8 ± 26.0 μm) compared to females (66.7 ± 24.5 μm), as well as similar perivenule capillary-free zone (42.5 ± 13.8 μm, 42.9 ± 15.0 μm, respectively for males and females), $F_{(1, 998)} = 0.13$, $P = 0.72$ (Fig. 6). The average linear extent of the perivenule capillary-free zone is 1.38 of a 3-mm venule length from our data.

For our normal subjects, the regression between retinal eccentricity and the periarteriole capillary-free zone was not significant ($F_{[3, 996]} = 0.834$, $P = 0.48$ with an R^2 of 0.003) for a multiple linear regression predicting periarteriole capillary-free zone based on arteriole distance from foveal center, arteriole diameter, and sex. Within the multiple linear regression, the influence of arteriole distance from foveal center ($P = 0.16$), arteriole diameter ($P = 0.98$), and sex ($P = 0.65$) were all not significant. The regression weights and subgroup means are summarized in the Table.

TABLE. Multiple Linear Regression Between Periarteriole and Perivenule Capillary-Free Zones and Vessel Distance from Fovea, Vessel Diameter, and Sex

	β	Mean ± SD (μm)	*t*	*P* Value
Periarteriole capillary-free zone				
Arteriole distance from fovea	0.36		1.41	0.16
Close (8°–12°)		68.6 ± 11.9		
Middle (12°–16°)		64.6 ± 12.7		
Far (16°–20°)		70.8 ± 14.8		
Arteriole diameter	−0.001		−0.025	0.98
Greater than 102 μm (average)		65.9 ± 13.7		
Less than 102 μm (average)		68.5 ± 12.5		
Sex	−0.737		−0.452	0.65
Perivenule capillary-free zone				
Venule distance from fovea	0.571		2.93	0.003
Close (8°–12°)		41.8 ± 0.38		
Middle (12°–16°)		40.2 ± 5.73		
Far (16°–20°)		46.6 ± 3.38		
Venule diameter	0.037		1.98	0.048
Greater than 129 μm (average)		43.5 ± 5.33		
Less than 129 μm (average)		41.1 ± 4.93		
Sex	0.259		0.286	0.78

Subgroup means are shown.

Investigative Ophthalmology & Visual Science

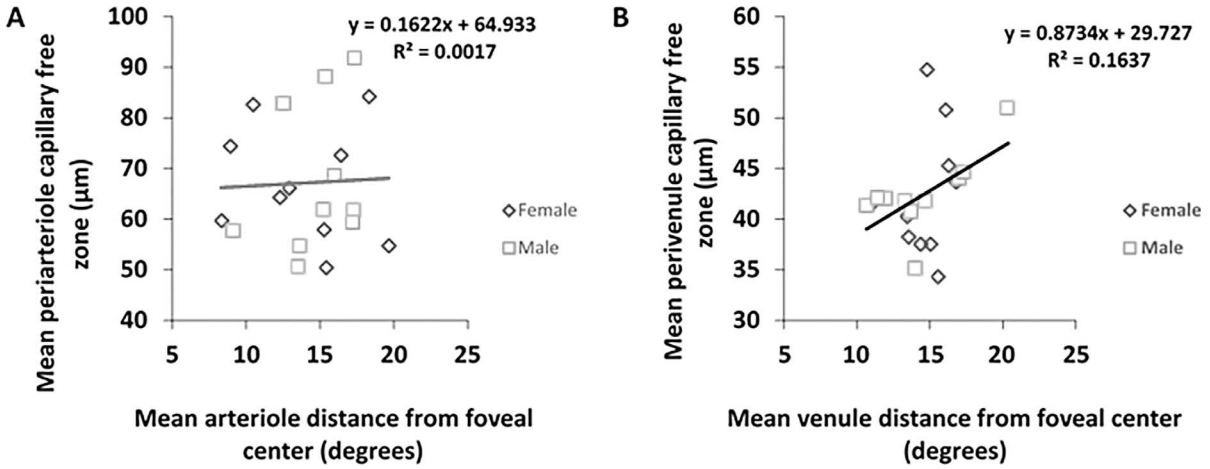

Figure 7. Mean periarteriole and perivenule capillary-free zones plotted as a function of mean arteriole and venule distances from foveal center, respectively. (**A**) Plot showing no association between mean periarteriole capillary-free zone and mean arteriole distance from foveal center, $\beta = 0.36$, $P = 0.16$. (**B**) Plot showing a positive association between mean perivenule capillary-free zone and mean venule distance from foveal center, $\beta = 0.571$, $P = 0.003$.

In contrast, the regression between retinal eccentricity and perivenule capillary-free zone was significant ($F_{[3, 996]} = 5.62$, $P = 0.001$ with an R^2 of 0.017) for a multiple linear regression predicting perivenule capillary-free zone based on venule distance from the foveal center, venule diameter, and sex. Predicted perivenule capillary-free zone = 29.1 + 0.571 (venule distance from the foveal center) + 0.037 (venule diameter) + 0.259 (sex). Venule distance from the foveal center ($P = 0.003$), and venule diameter ($P = 0.048$) were significant, but sex ($P = 0.78$) was not significant.

Thus, there was no significant association between periarteriole capillary-free zone and arteriole distance from foveal center (Fig. 7A) but there was a positive association between perivenule capillary-free zone and venule distance from the foveal center. For a 300 μm (~1°) increase in venule distance from foveal center, the perivenule capillary-free zone increases by 0.571 μm holding all other variables constant (Fig. 7B). There was also no significant association between periarteriole capillary-free zone and arteriole diameter (Fig. 8A), but there was a positive association between perivenule capillary-free zone and venule diameter. For a 1-μm increase in venule diameter, perivenule capillary-free zone increases by 0.037 μm holding all other variables constant (Fig. 8B).

There was no significant association between mean periarteriole capillary-free zone and FAZ effective diameter, $r = -0.167$, $P = 0.48$ (Fig. 9A). There was also no significant association between mean perivenule capillary-free zone and FAZ effective diameter, $r = -0.196$, $P = 0.41$ (Fig. 9B). Mean periarteriole capillary-free zone was not significantly associated with mean perivenule capillary-free zone, $r = 0.244$, $P = 0.30$. However, there was a significant positive association between asymmetry indices and FAZ effective diameter, $r = 0.49$, $P = 0.028$ (Fig. 9C). There was also no significant association between FAZ size and age, $r = 0.189$, $P = 0.43$, although our age range was so narrow that this would be expected. The average FAZ of all subjects was 0.368 ± 0.114 mm^2. The mean asymmetry indices and effective diameter of all subjects was 0.957 ± 0.130, and 674 ± 120 μm respectively. The FAZ of males (0.350 ± 0.142 mm^2) did not differ from that of females (0.386 ± 0.082 mm^2), $t(18) = 0.50$, as would be expected for a small sample size. The coefficient of variation (CV) of the FAZ (0.311) did not differ from that of the periarteriole (0.376) and perivenule (0.337) capillary-free zones, $F_{(19,19)} = 1.47$, $P = 0.21$, $F_{(19,19)} = 1.18$, $P = 0.36$, respectively. A similar trend was found for the CV of the periarteriole versus perivenule capillary-free zones, $F_{(19,19)} = 1.25$, $P = 0.32$.

In the individual with diabetes, we also observed focal remodeling of the capillary-free zones, including the FAZ, periarteriole capillary-free zone, and perivenule capillary-free zone (Figs. 10A, 10B). As expected, the FAZ had an irregular shape. The FAZ_H was 860 μm and the FAZ_V was 781 μm, larger than the mean from the effective diameter of the controls (674 μm) but not outside the 95% 1-tailed confidence limit of 881 μm. There are clear microaneurysms and small regions of vessel remodeling, which were not limited to the FAZ (Fig. 10A). There were also regions of nonperfused or poorly perfused perifoveal capillaries, as well as regions near both inferior arterioles and venules that were conspicuously dark (i.e., lacking capillaries with perfusion rates above the criterion for OCTA; Figs. 10A, 10B).

The mean periarteriole capillary-free zone is 106 μm, which is greater than the average periarteriole capillary-free zone of the controls (67.2 μm) and outside the right sided one-tailed 95% confidence limit (68.6 μm) of the healthy controls. This was computed for an arteriole distance from the fovea of 15.5° and an arteriole diameter of 81 μm, which are both less than or within the one tailed 95% confidence limit of 15.4° and 107 μm, respectively, for arteriole distance and diameter for the healthy controls. The linear distance of sampling at regular or evenly spaced intervals is 3.30 mm.

The mean perivenule capillary-free zone is 79.6 μm, which is greater than the average perivenule capillary-free zone of the controls (42.7 μm) and outside the one-tailed 95% confidence limit (43.5 μm) of the healthy controls. This was computed for a venule distance from the fovea of 15.2° and a venule diameter of 134 μm, which are both less than or within the one-tailed 95% confidence limit of 15.5° and 136 μm respectively, for venule distance and diameter for the healthy controls. The linear distance of sampling at regular or evenly spaced intervals is 3.20 mm.

Using the multiple regression parameters from controls (Table), we computed the expected perivenule capillary-free zone, perivenule CFZ = 29.1 + 0.571 (15.2) + 0.037 (134) + 0.259 (2) = 43.3 μm. The 95%, 1-tail confidence limit (18 degrees of freedom) based on the standard deviation of the residuals from the multiple regression gives a cutoff of 58.9 μm. Thus, the measured perivenule capillary-free zone (79.6 μm) of the diabetic subject in Figure 10 is significantly greater

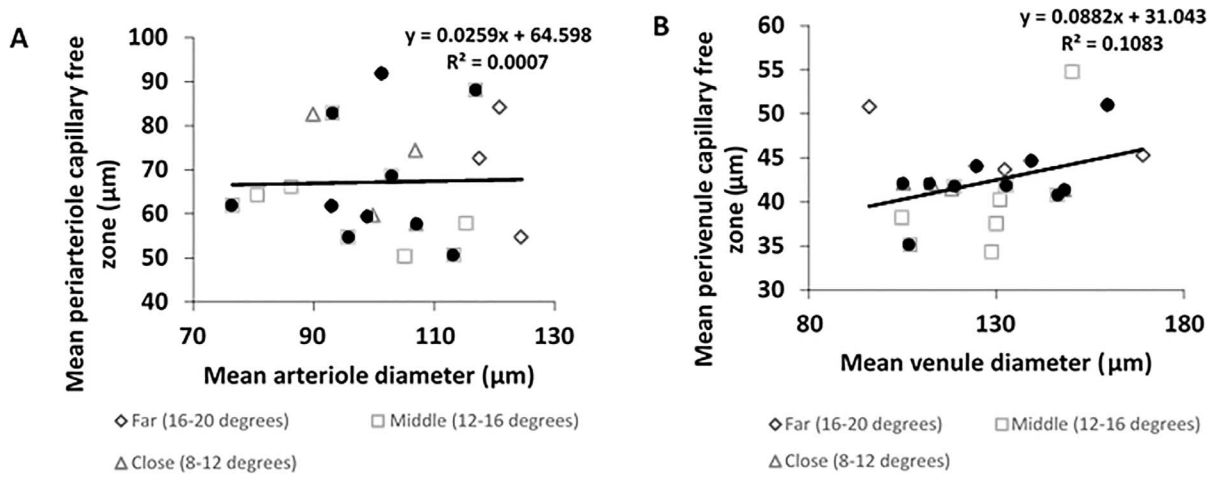

Figure 8. Mean periarteriole and perivenule capillary-free zones plotted as a function of mean arteriole and venule diameter, respectively. (**A**) Plot showing no association between mean periarteriole capillary-free zone and mean arteriole diameter, $\beta = -0.001$, $P = 0.98$. (**B**) Plot showing a positive association between mean perivenule capillary-free zone and mean venule diameter, $\beta = 0.037$, $P = 0.048$. *Closed* and *open* symbols represent male and female, respectively.

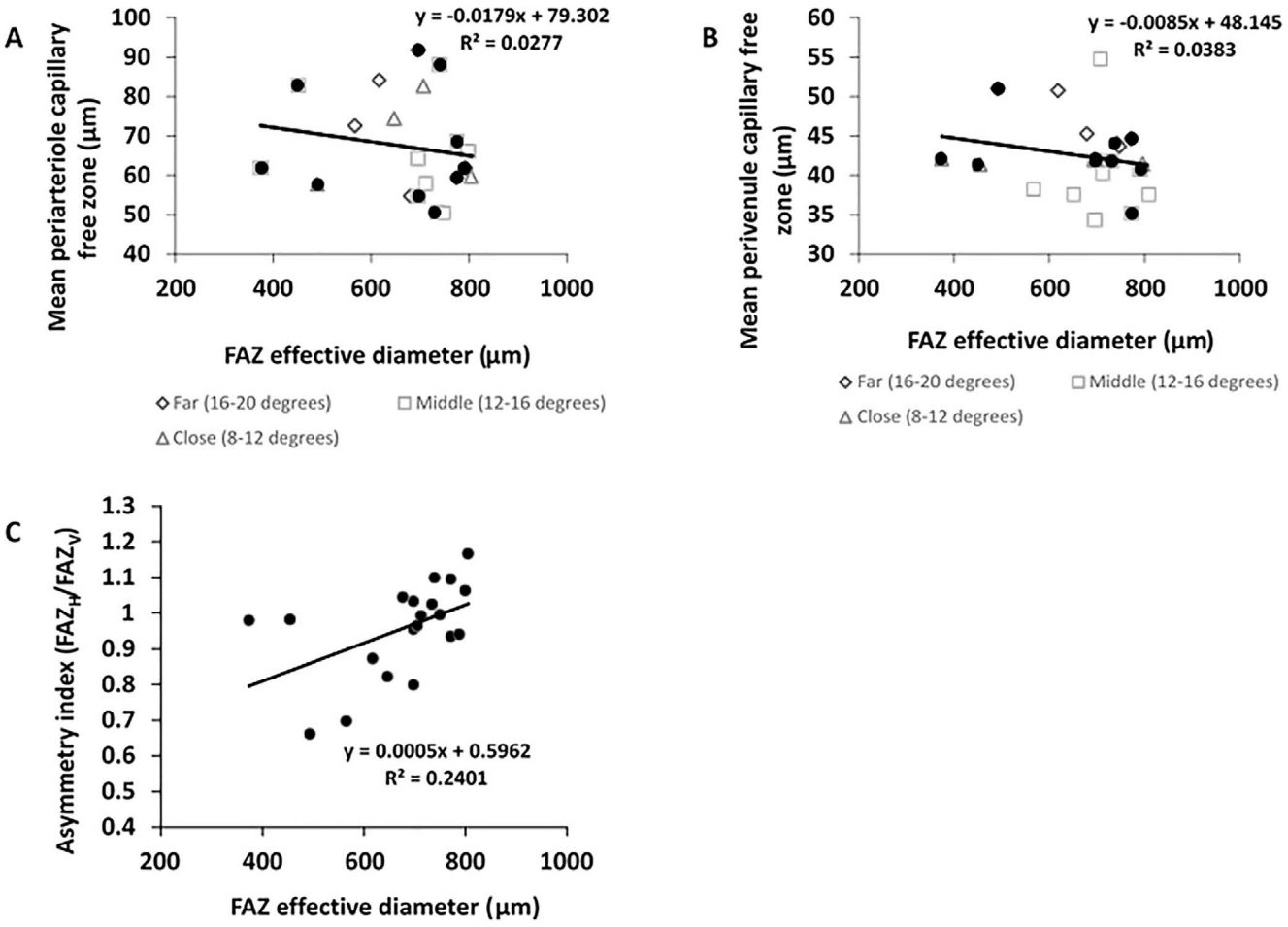

Figure 9. Mean periarteriole capillary-free zone, mean perivenule capillary-free zone, and asymmetry indices plotted as a function of FAZ effective diameter. (**A**) Plot of mean periarteriole capillary-free zone versus FAZ effective diameter showing lack of significant association, $r = -0.167$, $P = 0.48$. (**B**) Plot of mean perivenule capillary-free zone versus FAZ effective diameter showing lack of significant association, $r = -0.196$, $P = 0.41$. (**C**) Plot of asymmetry indices versus FAZ effective diameter showing a significant positive association, $r = 0.49$, $P = 0.028$ indicating that the shape of the FAZ area is horizontally elongated with a large FAZ area, but vertically elongated with a small FAZ area. *Closed* and *open symbols* represent male and female, respectively.

Investigative Ophthalmology & Visual Science

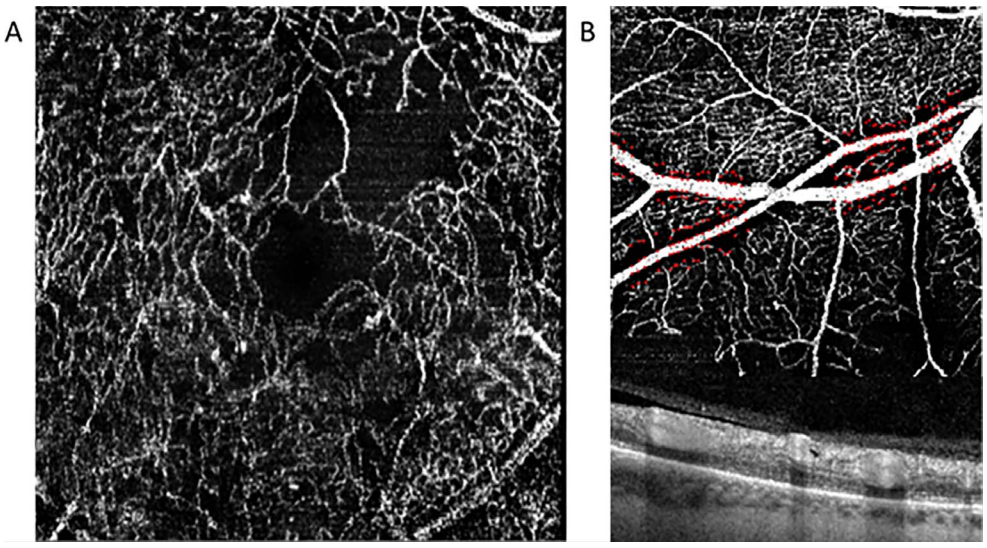

Figure 10. OCTA and OCT data of a type 2 diabetic participant showing variable remodeling of capillary-free zones, in a retina that is thin. (**A**) Remodeling of the microvasculature including nonperfusion or slowed perfusion of the capillary free zone in the fovea (FAZ) and also in the perifoveal region, plus microaneurysms, in 10° × 10° OCTA results from both plexuses in a 54-year-old diabetic female. (**B**) Top- irregular capillary-free zones, appearing larger than in control subjects, with sampled points plotted to show sampled linear distance around an inferior retina arteriole (15.5° from foveal center) and venule (15.2° from foveal center), as well as additional microaneurysms. *Bottom* B-scan corresponding to OCTA data, demonstrating that the patient has a thin retina.

than predicted from healthy control subjects with similar parameters.

Discussion

This study used two noninvasive imaging modalities (OCTA and AOSLO) to image and quantify FAZ parameters, periarteriole, and perivenule capillary-free zones in young healthy subjects (Figs. 1–5) and provided evidence of potential remodeling in diabetics (Fig. 10). All of our young, healthy subjects had readily quantifiable periarteriole and perivenule capillary-free zones, with a wide selection of regions of interest for potential measurements. In agreement with previous studies,[32–34] periarteriole capillary-free zones were clearly visualized and quantified. Perivenule capillary-free zones were also measured, consistent with one previous study[34] but in contrast to other studies failing to measure it.[32,33] Our finding of periarteriole capillary-free zones as being wider than perivenule capillary-free zones is also consistent with the results of a previous study.[34] Our results also show that venule distance from foveal center, and diameter are significantly predictive of the perivenule capillary-free zones. Thus, previous studies may have had insufficient resolution or contrast to delineate perivenule capillary-free zones, particularly with FA and the inability to restrict measurements to a narrow axial range, or may have measured too close to the fovea. Measurement of capillary-free zones provides a wide range of measurement locations (Figs. 1, 2), unlike the FAZ.

Our finding of the periarteriole capillary-free zone being wider than the perivenule capillary-free zone in the healthy retina is consistent with the retinal arterioles carrying oxygenated blood in the healthy retina and hence a reduced need for capillaries to exist immediately around the arterioles.[32] However, the healthy retina extracts oxygen and the venules are at a lower level of oxygenation and hence there is an increased need for the capillaries to exist closer to the venules.[33] The retinal veins however do carry oxygen, and the larger veins provide a larger reservoir, as well as a large surface area, for oxygen diffusion and hence, the increase in the perivenule capillary-free zones with increasing lumen diameter of the venules was observed. Also, the larger perivenule capillary-free zones observed at larger distances from the fovea may be due to lower cell density farther away from the fovea and hence less metabolic demand in these regions.

The FAZ, periarteriole, and perivenule capillary-free zones varied from one normal subject to another. Our results show that smaller FAZ sizes are associated with vertically elongated FAZ while larger FAZ sizes are associated with a horizontally elongated FAZ (Fig. 9C), consistent with our previous AOSLO study.[6] The human FAZ is not fully formed until after approximately 6 years of life.[52,53] The development of the FAZ and lateral displacement of the inner retinal neurons during this period of development has been tied to mechanical stress caused by eye growth and intraocular pressure.[54] The relation between shape and size of the FAZ has been suggested to arise as a result of variation in mechanical stress during the formation of the foveal pit.[6] This interindividual variability, including the relation between the size and shape of the FAZ, may have led to our finding of no association of FAZ and the periarteriole or perivenule capillary-free zone (Figs. 9A, 9B). However, the area of the FAZ varies strikingly with DR, with patients having FAZ areas more than twice that of controls.[15] Newer analyses approaches for FAZ are under development that incorporate a larger area of the retina, thus including more vessels and reducing the increased inter-subject variability contributed by developmental differences and a limited number of sampled vessels available in the FAZ inner loop.[55] The mean FAZ of our young healthy subjects using OCTA (0.368 ± 0.114 mm^2) was comparable to that measured with AOSLO in our previous study and another study; (0.32 ± 0.16 mm^2)[6] and (0.323 ± 0.107 mm^2)[56] as well as with another OCTA study (0.335 ± 0.113 mm^2)[26] and two other studies with FA; (median = 0.35 mm^2),[12] and (0.367 ± 0.090 mm^2).[57] The FAZ effective diameter of our young normal subjects (674 ± 120 μm) was also comparable to that found with AOSLO in our previous study and another study; (614 ± 184 μm),[6] and (633 ± 103 μm).[56]

The good agreement between AOSLO and OCTA was found in normal subjects and thus in retinal vessels that did not

include vessel remodeling. We measured to the center of capillaries, not the edges. The OCTA measurements provided sufficiently narrow confidence limits to allow comparisons of a single individual to the model from a group of controls. However, in this population and with this method, the lack of high lateral resolution of OCTA was not the disadvantage that it might be in the presence of extensive vessel remodeling. AOSLO can help distinguish among vessels within capillary tangles.[38] However, it is not yet known if AOSLO will be necessary to reduce noise in the capillary-free zone measurements. From a clinical perspective, extensive vascular remodeling seen on either technique, or large non-perfused areas, already indicate pathological changes. Further, vascular remodeling, such as in Figure 10, can be focal and variable over the retina. OCTA provides a wider field of view than does AOSLO. The large, black areas indicating lack of perfused capillaries are readily detected as on maps from either technique. It is not yet known how sensitive either technique is alone or whether a combination provides additional accuracy or more samples that are useful clinically.

Retinal vascular changes in DR are complex and often unexpected by clinical classification, and include capillary nonperfusion, capillary tangles, and the formation of arteriovenous shunts.[38] There can be a paradoxical higher oxygen saturation in venules due to reduced oxygen extraction from the retina.[10,11] Vessel remodeling, as well as other vascular changes such as microaneurysms, can all reduce the ability to quantify the FAZ, the periarteriole, or perivenule capillary-free zones. Capillary nonperfusion or dropout around arterioles may also occur and hence lead to a larger FAZ, periarteriole, or perivenule capillary-free zones in diabetics, as shown in Figure 10. Thus, the capillary-free zones around the arterioles and venules may serve as a biomarker which may aid in the diagnosis, management, and monitoring of disease progression in DR. The developed capillary-free zone is not limited to the perivenule or periarteriole region, but might be more readily detected due to the contrast. As the present study is a cross-sectional study in young control subjects, the next step would be to assess the mean periarteriole and perivenule capillary-free zones over time and in a wider range of control subjects, to serve as a baseline against which values in patients could be measured as indicative of diabetic retinopathy (DR) classification and progression. The qualitative grading as well as quantitative metrics such as width of the capillary-free zones may also aid in staging DR since it is well established that there can be retinal changes more severe than seen on clinical exam or fundus photography.[7,38,44] The capillary-free zones, both periarteriole and perivenule, along with more advanced metrics concerning capillaries near the fovea,[45,46] and other measures, may aid in bringing us closer to the needed reclassification of DR that is now possible with improved imaging modalities.

OCTA and AOSLO have the ability to generate vascular maps of a specific vascular plexus, and an emphasis in recent studies with OCTA concerns normative values and types of artifact removal for quantifying the vascular plexuses at different depths, such as the SVP and DVP.[4,39–42] In our study, we reported data only for the SVP capillary-free zones outside of the fovea, since this is where the larger vessels occur, and capillary-free zones would be expected.[35]

To understand what sizes and locations of capillary-free zones indicate the highest risk for retinal damage, further research is needed to form a 3D model of oxygen demand and potential ischemia. A complete model would include such variables for each measurement location as retinal thickness, number of capillary layers, distance travelled for a given arteriole or venule, along with our present variables of vessel diameter and distance from the fovea that were statistically significant for venules. Further refinement of patient demographics (e.g., age), available oxygen (i.e., beyond classification of vessels as an artery or vein), and other factors are also needed for a complete model.

The periarteriole and perivenule capillary-free zones also offer the potential for measurements focally over a large region of retina. However, our OCTA system has remaining issues with projection artifacts. Hence, cleanly visualizing vascular plexuses at different depths without interference of neighboring plexuses was difficult. However, this is unlikely to affect our results, since we did not measure capillary density. Also, we measured the capillary-free zones in the SVP, which does not have overlying vasculature. Measuring capillary-free zones may not be accurate in the DVP with OCTA,[35] plus there are not large retinal vessels to lead to such zones. Projection artifacts from more superficial arterioles and venules in the SVP as well as deeper capillaries having a more lobular pattern, make identification of zone more difficult in the DVP. Patient eye movement and alignment decreased contrast in two images, but in all subjects, periarteriole and perivenule capillary-free zones were clearly observed and quantifiable.

In summary, using two noninvasive imaging modalities (OCTA and AOSLO), our results provide evidence that periarteriole and perivenule capillary-free zones both exist in the SVP, with the former significantly wider than the latter in all normal subjects. This is consistent with the healthy retina having arterioles carrying oxygen-rich blood that diffuses to support the retina. The healthy retina then extracts oxygen, and thus capillaries are needed nearer to the venules to overcome the lower proportion of oxygen available to diffuse. Venule distance from foveal center and diameter are predictive of the width of the perivenule capillary-free zone, but a full 3D model would include retinal thickness. In DR, there can be initial abnormally high oxygen saturation in the venules, and there is also capillary nonperfusion or dropout. These are consistent with the irregular and larger capillary-free zones around the arterioles and venules shown for our diabetic subject. This occurs also for the FAZ, but using the FAZ alone is influenced by interindividual variability with FAZ size prior to disease onset: a large FAZ size is associated with horizontal elongation of the FAZ and a small FAZ size is associated with a vertical elongation of the FAZ. The capillary-free zones may be explored in future studies as possible tools for the diagnosis of retinal vascular diseases, as the baseline measurements provided in this study may be compared against values found in patients.

Acknowledgments

Supported by STTR EY026105 (AEE, MSM, SAB) and EY028499 (AEE) and NIH EY024315 (SAB)

Disclosure: **E. Arthur**, None; **A.E. Elsner**, Aeon Imaging, LLC (I, S) P; **K.A. Sapoznik**, None; **J.A. Papay**, None; **M.S. Muller**, Aeon Imaging, LLC (I, S) P; **S.A. Burns**, None

References

1. Lechner J, O'Leary OE, Stitt AW. The pathology associated with diabetic retinopathy. *Vision Res*. 2017;139:7–14.
2. Antonetti DA, Klein R, Gardner TW. Diabetic retinopathy. *N Engl J Med*. 2012;29:1227–1239.
3. Burns SA, Elsner AE, Sapoznik KA, Warner RL, Gast TJ. Adaptive optics imaging of the human retina. *Prog Retin Eye Res*. 2019;68:1–30.
4. de Carlo TE, Romano A, Waheed NK, Duker JS. A review of optical coherence tomography angiography (OCTA). *Int J Retina Vitreous*. 2015;1:5.

5. Nesper PL, Soetikno BT, Zhang HF, Fawzi AA. OCT angiography and visible-light OCT in diabetic retinopathy. *Vision Res*. 2017;139:191–203.
6. Chui TYP, VanNasdale DA, Elsner AE, Burns SA. The association between the foveal avascular zone and retinal thickness. *Invest Ophthalmol Vis Sci*. 2014;55:6870–6877.
7. Tam J, Dhamdhere KP, Tiruveedhula P, et al. Disruption of the retinal parafoveal capillary network in type 2 diabetes before the onset of diabetic retinopathy. *Invest Ophthalmol Vis Sci*. 2011;52:9257–9266.
8. Choi W, Waheed NK, Moult EM, et al. Ultrahigh speed swept source optical coherence tomography angiography of retinal and choriocapillaris alterations in diabetic patients with and without retinopathy. *Retina*. 2017;37:11–21.
9. Gardiner TA, Archer DB, Curtis TM, Stitt AW. Arteriolar involvement in the microvascular lesions of diabetic retinopathy: implications for pathogenesis. *Microcirculation*. 2007; 14:25–38.
10. Stitt AW, Curtis TM, Chen M et al. The progress in understanding and treatment of diabetic retinopathy. *Prog Retin Eye Res*. 2016;51:156–186.
11. Hammer M, Vilser W, Riemer T, et al. Diabetic patients with retinopathy show increased retinal venous oxygen saturation. *Graefes Arch Clin Exp Ophthalmol*. 2009;247:1025–1030.
12. Bresnick GH, Condit R, Syrjala S, Palta M, Groo A, Korth K. Abnormalities of the foveal avascular zone in diabetic retinopathy. *Arch Ophthalmol*. 1984;102:1286–1293.
13. Leite E, Mota MC, Faria DA et al. Quantification of the foveolar zone in normal and diabetic patients. *J Fr Ophtalmol*. 1988; 12:665–668.
14. Arend O, Wolf S, Jung F et al. Retinal microcirculation in patients with diabetes mellitus: dynamic and morphological analysis of perifoveal capillary network. *Br J Ophthalmol*. 1991;75:514–518.
15. Arend O, Wolf S, Harris A, Reim M. The relationship of macular microcirculation to visual acuity in diabetic patients. *Arch Ophthalmol*. 1995;113:610–614.
16. Arend O, Remky A, Evans D, Stüber R, Harris A. Contrast sensitivity loss is coupled with capillary dropout in patients with diabetes. *Invest Ophthalmol Vis Sci*. 1997;38:1819–1824.
17. Arend O, Wolf S, Remky A, et al. Perifoveal microcirculation with non-insulin-dependent diabetes mellitus. *Graefes Arch Clin Exp Ophthalmol*. 1994;232:225–231.
18. Laatikainen L, Larinkari J. Capillary-free area of the fovea with advancing age. *Invest Ophthalmol Vis Sci*. 1977;16:1154–1157.
19. Mendis KR, Balaratnasingam C, Yu P, et al. Correlation of histologic and clinical images to determine the diagnostic value of fluorescein angiography for studying retinal capillary detail. *Invest Ophthalmol Vis Sci*. 2010;51:5864–5869.
20. Conrath J, Giorgi R, Raccah D, Ridings B. Foveal avascular zone in diabetic retinopathy: quantitative vs qualitative assessment. *Eye (Lond)*. 2005;19:322–326.
21. Wu L, Huang Z, Wu D, Chan E. Characteristics of the capillary-free zone in the normal human macula. *Jpn J Ophthalmol*. 1985;29:406–411.
22. Wolf S, Wald K, Elsner AE, Staurenghi G. Indocyanine green choroidal video angiography: a comparison of imaging analysis with the laser ophthalmoscope and the fundus camera. *Retina*. 1993;13:266–269.
23. Takase N, Nozaki M, Kato A, Ozeki H, Yoshida M, Ogura Y. Enlargement of foveal avascular zone in diabetic eyes evaluated by en face optical coherence tomography angiography. *Retina*. 2015;35:2377–2383.
24. Iafe NA, Phasukkijwatana N, Chen X, Sarraf D. Retinal capillary density and foveal avascular zone area are age-dependent: quantitative analysis using optical coherence tomography angiography. *Invest Ophthalmol Vis Sci*. 2016; 57:5780–5787.
25. Samara WA, Say EA, Khoo CT et al. Correlation of foveal avascular zone size with foveal morphology in normal eyes using optical coherence tomography angiography. *Retina*. 2015;35:2188–2195.
26. Gong D, Zou X, Zhang X, Yu W, Qu Y, Dong F. The influence of age and central foveal thickness on foveal zone size in healthy people. *Ophthalmic Surg Lasers Imaging Retina*. 2016;47:142–148.
27. Krawitz BD, Mo S, Geyman LS, et al. Acircularity index and axis ratio of the foveal avascular zone in diabetic eyes and healthy controls measured by optical coherence tomography angiography. *Vision Res*. 2017;139:177–186.
28. Muller MS, Elsner AE. Confocal retinal imaging using a digital light projector with a near infrared VCSEL source. *Proc SPIE Int Soc Opt Eng*. 2018;10546:105460G.
29. Bradley A, Zhang H, Applegate RA, Thibos LN, Elsner AE. Entoptic image quality of the retinal vasculature. *Vision Res*. 1998;38:2685–2696.
30. Arthur E, Papay JA, Haggerty BP, Clark CA, Elsner AE. Subtle changes in diabetic retinas localised in 3D using OCT. *Ophthalmic Physiol Opt*. 2018;38:477–491.
31. Ferris FL 3rd. The importance of peripheral diabetic retinopathy. *Ophthalmology*. 2015;122:869–870.
32. Asdourian GK, Goldberg MF. The angiographic pattern of the peripheral retinal vasculature. *Arch Ophthalmol*. 1979;97: 2316–2318.
33. Michaelson IC. *Retinal Circulation in Man and Animals*. Vail, Derrick ed. Springfield, IL: Charles C Thomas; 1954.
34. Toussaint D, Kuwabara T, Cogan DG. Retinal vascular patterns: Part II. Human retinal vessels studied in three dimensions. *Arch Ophthalmol*. 1961;65:575–581.
35. Balaratnasingam C, An D, Sakurada Y, et al. Comparisons between histology and optical coherence tomography angiography of the periarterial capillary-free zone. *Am J Ophthalmol*. 2018;189:55–64.
36. Hartnett ME eds. *Pediatric Retina*. Philadelphia: Lippincott Williams & Wilkins; 2005:9.
37. Werkmeister RM, Schmidl D, Aschinger G, et al. Retinal oxygen extraction in humans. *Sci Rep*. 2015;27:15763.
38. Burns SA, Elsner AE, Chui TY et al. In vivo adaptive optics microvascular imaging in diabetic patients without clinically severe diabetic retinopathy. *Biomed Opt Express*. 2014;5: 961–974.
39. Spaide RF, Klancnik JM, Cooney MJ. Retinal vascular layers imaged by fluorescein angiography and optical coherence tomography angiography. *JAMA Ophthalmol*. 2015;133:45–50.
40. Zhang M, Hwang TS, Dongye C, Wilson DJ, Huang D, Jia Y. Automated quantification of nonperfusion in three retinal plexuses using projection-resolved optical coherence tomography angiography in diabetic retinopathy. *Invest Ophthalmol Vis Sci*. 2016;57:5101–5106.
41. Campbell JP, Zhang M, Hwang TS, et al. Detailed vascular anatomy of the human retina by projection-resolved optical coherence tomography angiography. *Scientific Rep*. 2017;7: 42201.
42. Zhang M, Hwang TS, Campbell JP, et al. Projection-resolved optical coherence tomographic angiography. *Biomed Opt Express*. 2016;7:816–828.
43. Elsner AE, Burns SA, Weiter JJ, Delori FC. Infrared imaging of sub-retinal structures in the human ocular fundus. *Vision Res*. 1996;36:191–205.
44. Elsner AE, Burns SA, Lobes LA Jr, Doft BH. Cone photopigment bleaching abnormalities in diabetes. *Invest Ophthalmol Vis Sci*. 1987;28:718–724.

Investigative Ophthalmology & Visual Science

45. Gia Y, Simonett JM, Wang J, et al. Evaluation of automatically quantified foveal avascular zone metrics for diagnosis of diabetic retinopathy using optical coherence tomography angiography. *Invest Ophthalmol Vis Sci*. 2018;59:2212–2221.
46. Ashraf M, Nesper PL, Jampol LM, Yu F, Fawzi AA. Statistical model of optical coherence tomography angiography parameters that correlate with severity of diabetic retinopathy. *Invest Ophthalmol Vis Sci*. 2018;59:4292–4298.
47. Faul F, Erdfelder E, Buchner A, Lang AG. Statistical power analyses using G* Power 3.1: Tests for correlation and regression analyses. *Behav Res Methods*. 2009;41:1149–1160.
48. Sapoznik KA, Luo T, De Castro A, Sawides L, Warner RL, Burns SA. Enhanced retinal vasculature imaging with a rapidly configurable aperture. *Biomed Opt Express*. 2018;9:1323–1333.
49. Hillard JG, Gast TJ, Chui TY, Sapir D, Burns SA. Retinal arterioles in hypo-, normo-, and hypertensive subjects measured using adaptive optics. *Trans Vis Sci Tech*. 2016;5(4):16.
50. Huang G, Zhong Z, Zou W, Burns SA. Lucky averaging: quality improvement of adaptive optics scanning laser ophthalmoscope images. *Opt Lett*. 2011;36:3786–3788.
51. Chui TY, Zhong Z, Song H, Burns SA. Foveal avascular zone and its relationship to foveal pit shape. *Optom Vis Sci*. 2012;89:602–610.
52. Snodderly DM, Weinhaus RS. Retinal vasculature of the fovea of the squirrel monkey, Saimiri sciureus: three-dimensional architecture, visual screening, and relationships to the neuronal layers. *J Comp Neurol*. 1990;297:145–163.
53. Snodderly DM, Weinhaus RS, Choi JC. Neural-vascular relationships in central retina of Macaque monkeys (Macaca fascicularis). *J Neurosci*. 1992;12:1169–1193.
54. Springer AD, Hendrickson AE. Development of the primate area of high acuity, 1: use of finite element analysis models to identify mechanical variables affecting pit formation. *Vis Neurosci*. 2004;21:53–62.
55. Lu Y, Simonett JM, Wang J, et al. Evaluation of automatically quantified foveal avascular zone metrics for diagnosis of diabetic retinopathy using optical coherence tomography angiography. *Invest Ophthalmol Vis Sci*. 2018;59:2212–2221.
56. Tam J, Martin JA, Roorda A. Noninvasive visualization and analysis of parafoveal capillaries in humans. *Invest Ophthalmol Vis Sci*. 2010;51:1691–1698.
57. Sander B, Larsen M, Engler C, Lund-Andersen H, Parving H-H. Early changes in diabetic retinopathy: capillary loss and blood-retina barrier permeability in relation to metabolic control. *Acta Ophthalmol*. 1994;72:553–559.

Investigative Ophthalmology & Visual Science